Fluid Phase Equilibria 581 (2024) 114076

Contents lists available at ScienceDirect

Fluid Phase Equilibria

journal homepage: www.journals.elsevier.com/fluid-phase-equilibria

Volumetric properties of three nonylphenol ethoxylated nonionic surfactant mixtures with methanol: Experimental study and modeling with Tammann-Tait and PC-SAFT equation of state

Moacir Frutuoso Leal da Costa, Hugo Andersson de Medeiros, Alanderson Arthu Araújo Alves, Lucas Henrique Gomes de Medeiros, Filipe Xavier Feitosa, Hosiberto Batista De Sant'Ana *

Grupo de Pesquisa em Termofluidodinâmica Aplicada, Departamento de Engenharia Química, Centro de Tecnologia, Universidade Federal do Ceará, Campus do Pici, Bloco 709 60455-760 Fortaleza-CE, Brasil

ARTICLE INFO

Keywords:
Nonionic ethoxylated surfactant
Methanol
Volumetric data
PC-SAFT modeling

ABSTRACT

Although physicochemical properties are essential for production and equipment design in oil and gas industries, there is still a lack of data for some systems because of hazardous temperature and pressure conditions. This work provides a volumetric behavior study of three different mixtures composed of nonylphenol ethoxylated nonionic surfactant (IGEPAL CO-520, CO-630, and CO-720) + methanol in the entire mole fraction composition range for temperatures from 313.15 K to 413.15 K and pressures up to 100.0 MPa. These systems behave as a regular liquid, with a volume contraction predominance. It was observed that for high methanol molar content, there is an increase in the cohesive forces because of the ethoxylated chain increases in oxyethylene units. Nevertheless, it was observed that the hydrogen bonds between ether oxygens and hydroxyl hydrogens decrease by increasing temperature, as given by internal pressure data and PC-SAFT modeling. Besides, a new set of parameters for the PC-SAFT equation of state is provided to calculate volumetric and second-order derivative properties.

1. Introduction

Surfactants have a wide range of applications because of their main characteristic: a hydrophobic tail and a hydrophilic head (i.e., an amphiphilic compound). There are two main classes of surfactants: ionic and nonionic. Ionic surfactants have a polar head from an ion (cation or anion). Otherwise, a nonionic surfactant has a polar head originating from a highly associative group (e.g., hydroxyl or amines) [1,2]. Typically, the nonionic surfactant class is of great industrial interest because of its association with the so-called green chemistry related to faster biodegradability. For instance, the nonylphenol ethoxylated surfactants are especially interesting because of their lower toxicity due to the size of the polyethoxylated chain [3].

The upstream sector is surrounded by hazardous conditions with high pressure and temperature in deepwater reservoirs [4–6]. For this reason, surfactants are often injected to lower the interfacial tension in reservoir rocks [7] in an enhanced oil recovery (EOR) process, e.g., the injection of surfactant foams. Furthermore, surfactants are also employed as demulsifying agents [8] injected in oil production wells to maintain the flow.

Moreover, the surfactant cloud point is strictly related to temperature [9–13]. For this reason, short-chain alcohol is usually applied as a co-surfactant once it directly impacts the surfactant's phase behavior, expanding the monophasic region. For instance, methanol gives good results for such purposes [10,14]. Indeed, the mixtures of nonionic surfactant + alcohol have their scope of application for stabilized foams [15].

The alkylphenol ethoxylated surfactant (IGEPAL CO-520, CO-630, and CO-720) + methanol systems could lead to a high degree of associative interactions [16] being responsible for inaccurate process design, especially at high pressure and high temperature (HPHT) applications. Paiva et al. [16,17] studied the volumetric properties of nonylphenol ethoxylated nonionic surfactant (IGEPAL CO-520, CO-630, and CO-720) + ethanol [16] and toluene [17] systems at atmospheric pressure. However, to our knowledge, there is no experimental data for those systems at HPHT operational conditions.

For high associative systems, the statistical association fluid theory (SAFT) developed by Chapman et al. [18] and the equation of state

* Corresponding author.
E-mail address: hbs@ufc.br (H.B. De Sant'Ana).

https://doi.org/10.1016/j.fluid.2024.114076
Received 10 January 2024; Received in revised form 1 March 2024; Accepted 6 March 2024
Available online 10 March 2024

Table 1
General Information [CAS number, Chemical Formula, Mole Fraction Purity, Polymerization Degree Range (n), and Average Molecular Weight] of All Chemical Compounds Used in This Paper.

chemical compound	CAS number	chemical formula	purity	N^a	molecular weight, g/mol
Methanol	67–56–1	CH_3OH	0.998	–	32.04
IGEPAL CO-520	68,412–54–4	$(C_4H_4O)_nC_{15}H_{24}O$	0.999	~5	441.00[a]
IGEPAL CO-630	68,412–54–4	$(C_4H_4O)_nC_{15}H_{24}O$	0.999	9 – 10	617.00[a]
IGEPAL CO-720	68,412–54–4	$(C_4H_4O)_nC_{15}H_{24}O$	0.999	10.5 – 12	749.00[a]

[a] Values reported by Sigma-Aldrich

derived from that theory, the perturbed chain SAFT (PC-SAFT) [19] are widely used for volumetric properties prediction [20–27].

This work is part of a larger project called HyPresProper (High-Pressure Property), whose main objective is to study volumetric data and derived properties for systems with industrial interests. Here, pure methanol, pure IGEPAL (CO-520, CO-630, and CO-720), and their binary mixtures liquid volumetric behavior were experimentally determined over the entire methanol molar composition range for a temperature range of 313.0 K to 413.0 K and pressures up to 100 MPa. The data were correlated with the Tamman-Tait equation, and the following derivative properties were determined: isothermal compressibility, isobaric expansivity, and internal pressure. From these data, a new set of PC-SAFT parameters was obtained. Additionally, nonylphenol ethoxylated nonionic surfactant (IGEPAL CO-520, CO-630, and CO-720) derivative properties were estimated through PC-SAFT equation derivatives.

2. Materials and methods

2.1. Materials

Table 1 gives chemical information for all three non-ionic surfactants (IGEPAL CO-520, CO-630, and CO-720) and the methanol used in this work. Moreover, all chemicals were used without any further purification processes.

2.2. Experiments

2.2.1. Mixture preparation

The nonylphenol ethoxylated nonionic surfactant (IGEPAL CO-520, CO-630, and CO-720) + methanol mixtures were gravimetrically prepared at atmospheric pressure using a sealed tube test to prevent any methanol vaporization after weighting, performed using an electronic digital scale (Shimadzu, model AY220) with an accuracy of ± 0.0001 g. These mixtures were homogenized using a vortex mixer. After that, all sample tubes were immersed in an ultrasonic bath (Elmasonic S 60H) to prevent bubble formation. The combined uncertainty on the composition was estimated to be lower than 0.71%.

2.2.2. Density measurements

Density measurements were performed in a vibrating U-tube densimeter (DMA HPM by Vinci Technologies), the calibration procedure of which is detailed elsewhere [28,29]. Briefly, the DMA U-tube densimeter was calibrated using deionized water (resistivity of 18.2 ± 0.2 $M\Omega{\cdot}cm$ at 298.15 K) and nitrogen (White Martins/Brazil, nominal purity of 99.996 %). Afterward, the validation procedure was accomplished using toluene (Sigma Aldrich/USA, nominal purity 99.5%). The density calibration standard deviation was 0.58 kg·m^{-3}. The validation procedure showed an average variation of 0.07%. The apparatus was also validated with high-density liquids such as ionic liquids, with densities up to 1230.3 kg·m^{-3} [30,31]. The operating limits of the densimeter setup are 100.00 MPa and 473.15 K.

The pressure system was controlled using a syringe pump (Teledyne ISCO, with a standard uncertainty of ± 0.7 MPa), and the temperature was controlled using a circulating liquid bath (Julabo FP50/Germany), with an uncertainty of ± 0.01 K. The mixture was transferred to the densimeter using a high-pressure floating piston cell by Vinci Technologies.

The expanded uncertainty on density measurements ($U(\rho)$) was calculated considering different uncertainty sources, such as pressure, temperature, standard deviation in calibration, and average deviation with the calibration fluid [28,29]. The maximum value for $U(\rho)$ was 1.7 kg·m^{-3}, with 95 % confidence (k = 2). The calculation procedure is described in the Supplementary Material file.

2.2.3. Density correlation

Density data was correlated with the Tammann-Tait equation [32,33], which is widely used to correlate high-pressure density data for associating compounds [30,31,34], as given below:

$$\rho(T,\ P) = \frac{\rho_o(T)}{1 - C{\cdot}ln\left(\frac{B(T)+\ P}{B(T)+\ P_{ref}}\right)} \tag{1}$$

$$\rho_o(T) = a_o + a_1{\cdot}T + a_2{\cdot}T^2 \tag{2}$$

$$B(T) = b_0 + b_1{\cdot}T + b_2{\cdot}T^2 \tag{3}$$

where ρ_o is the temperature-dependent polynomial for the reference pressure (P_{ref} = 10MPa); a_0, a_1, and a_2 are fitting parameters for the density at the reference pressure; and, b_0, b_1, b_2, and C are fitting pa-

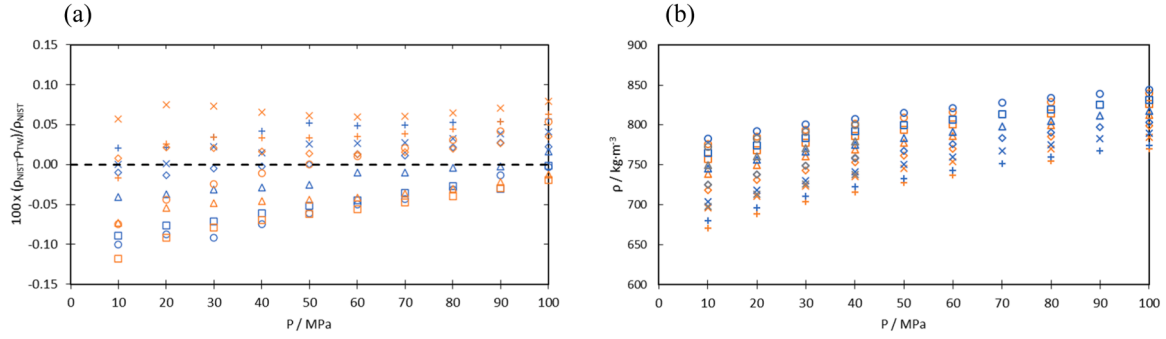

Fig. 1. (a) Pure methanol density measured (blue -) and Tammann-Tait calculation (orange -) in this work (TW), both data compared with NIST database at different temperatures, and (b) measured methanol density in this work (blue -) compared with literature data: Xiang and coworkers [49] (orange -) and Abdulagatov and coworkers [50] (grey -). Shapes in (a) are for temperatures: 313.15 K (○), 333.15 K (□), 353.15 K (Δ), 373.15 (◇), 393.15 K (x), 413.15 K (+). Orange shapes in (b) are 320.0 K (○), 340.0 K (□), 360.0 K (Δ), 380.0 (◇), 400.0 (x), 420.0 K (+). Grey shapes in (b) are 323.15 K (○), 348.15 K (Δ), 373.15 K (◇), and 398.15 (x).

Table 2
Tammann-Tait equation adjustable parameters were regressed for pure IGEPAL, pure methanol, and its mixtures studied in this work.

	Mixtures					
Parameters	IGE	IGE 80 – MetOH 20	IGE 60 – MetOH 40	IGE 40 – MetOH 60	IGE 20 – MetOH 80	MetOH
	IGEPAL CO – 520					
a_0(kg·m^{-3})	1274.8	1259.0	1235.8	1225.2	1162.4	884.02
a_1(kg·m^{-3}·K^{-1})	−0.8276	−0.7468	−0.6135	−0.6657	−0.4640	0.2112
a_2(kg·m^{-3}·K^{-2})	1.35E-04	9.82E-06	−2.09E-04	−1.46E-04	−4.94E-04	−1.71E-03
b_0(MPa)	546.67	515.70	490.24	504.79	458.36	316.70
b_1(MPa·K^{-1})	−1.6446	−1.4930	−1.3435	−1.504	−1.346	−1.012
b_2(MPa·K^{-2})	1.35E-03	1.15E-03	9.20E-04	1.17E-03	9.85E-04	7.51E-04
C	0.0872	0.0864	0.0858	0.0870	0.0879	0.0991
[a]%AARD (%)	3.66E-03	4.66E-03	4.05E-03	3.77E-03	3.53E-03	2.66E-02
[b]SD (kg·m^{-3})	6.88E-03	8.09E-03	6.53E-03	9.12E-03	5.18E-03	3.37E-02
	IGEPAL CO – 630					
$a_0(kg{\cdot}m^{-3})$	1306.52	1288.3	1272.9	1264.7	1211.20	
$a_1(kg{\cdot}m^{-3}{\cdot}K^{-1})$	−0.8803	−0.7843	−0.7426	−0.7457	−0.5841	
$a_2(kg{\cdot}m^{-3}{\cdot}K^{-2})$	1.85E-04	3.44E-05	−9.82E-06	−2.72E-05	−3.02E-04	
$b_0(MPa)$	574.34	566.90	475.91	524.00	486.15	
$b_1(MPa{\cdot}K^{-1})$	−1.7526	−1.7065	−1.2732	−1.5414	−1.4360	
$b_2(MPa{\cdot}K^{-2})$	1.48E-03	1.39E-03	8.57E-04	1.20E-03	1.09E-03	
C	0.0884	0.08715	0.0871	0.0879	0.0880	
[a]%AARD (%)	8.04E-03	3.81E-03	5.98E-03	3.65E-03	4.00E-03	
[b]SD (kg·m^{-3})	1.46E-02	6.83E-03	1.09E-02	5.93E-03	6.41E-03	
	IGEPAL CO – 720					
$a_0(kg{\cdot}m^{-3})$	1313.20	1309.10	1304.40	1269.80	1230.80	
$a_1(kg{\cdot}m^{-3}{\cdot}K^{-1})$	−0.8745	−0.8671	−0.8441	−0.7177	−0.6134	
$a_2(kg{\cdot}m^{-3}{\cdot}K^{-2})$	1.79E-04	1.69E-04	1.16E-04	−6.38E-05	−2.67E-04	
$b_0(MPa)$	599.73	5.81E+02	599.09	529.41	528.76	
$b_1(MPa{\cdot}K^{-1})$	−1.8449	−1.7922	−1.8561	−1.5601	−1.5853	
$b_2(MPa{\cdot}K^{-2})$	1.58E-03	1.54E-03	1.59E-03	1.23E-03	1.24E-03	
C	0.0892	0.08741	0.0886	0.0875	0.0896	
[a]%AARD (%)	3.57E-03	3.44E-03	4.36E-03	2.67E-03	3.56E-03	
[b]SD (kg·m^{-3})	6.26E-03	5.86E-03	7.03E-03	1.03E-02	5.78E-03	

[a] $\%AARD = \frac{100}{N_{data}} * \sum_{i-1}^{N_{data}} \left| \frac{\rho_i^{calc} - \rho_i^{exp}}{\rho_i^{exp}} \right|$.

[b] $SD = \frac{\sqrt{\sum_i (\rho_i^{calc} - \rho_i^{exp})^2}}{N_{data}}$. $U(\rho) = 1.7\ kg/m^3$.

rameters for the whole dataset. Derived properties obtained from the Tammann-Tait equation, such as isobaric expansivity (α_P) and isothermal compressibility (k_T), have a dependency on the reference pressure [35]. Therefore, the reference pressure was the minimum pressure that density was measured ($P_{ref} = 10\ MPa$), which was limited by methanol volatility in the conditions studied in this work; once above 333.15 K, the system was not in the monophasic region for the commonly used atmospheric pressure, and density measurements were not viable. This reference value was used only due to experimental constraints, and to validate the calculations performed in this work using the Tammann-Tait equation, the derivative properties obtained were compared with data available for methanol [36], resulting in an average absolute deviation (%*AARD*) of 1.78% for k_T and 5.95% for α_P [full shapes in Figs. 3(b) and 4 (b)].

The derived properties were estimated through the analytical derivative of the Tammann-Tait equation using the fitted parameters after their definitions [37], resulting in the expressions:

$$k_T = -\left(\frac{1}{\rho}\right)\cdot\left(\frac{\partial\rho}{\partial P}\right)_T = \frac{C}{\left(1 - C\cdot ln\left(\frac{B(T)+P}{B(T)+P_{ref}}\right)\right)\cdot(B(T)+P)} \tag{4}$$

$$\alpha_P = \left(\frac{1}{\rho}\right)\cdot\left(\frac{\partial\rho}{\partial T}\right)_P = -\frac{a_1 + 2\cdot a_2\cdot T}{\rho(T,P_{ref})} - \frac{C\cdot(P_{ref}-P)}{(B(T)+P)\cdot(B(T)+P_{ref})}\cdot\frac{b_1 + 2\cdot b_2\cdot T}{\left[1 - C\cdot ln\left(\frac{b(T)+P}{b(T)+P_{ref}}\right)\right]} \tag{5}$$

$$P_i = \left(\frac{\partial U}{\partial V}\right)_T = T\left(\frac{\partial P}{\partial T}\right)_V - P = T\frac{\alpha_P}{\kappa_T} - P \tag{6}$$

The isobaric expansivity and isothermal compressibility are critical parameters for better understanding the pressure and temperature effects on the associating systems' volumetric behavior. Also, the internal pressure indicates the nature of intermolecular interactions, increasing when hydrophobic interactions (repulsive forces) are predominant [38]. The Tammann-Tait parameters were fitted using the Levenberg-Marquardt algorithm [39], minimizing the absolute average deviation in Eq. (13). The expanded uncertainties ($k = 2$) in the derived properties were estimated to be: $U(\alpha_P) = 0.001\ K^{-1}$, $U(\kappa_T) = 4.2\ x\ 10^{-6}$ MPa^{-1}, and $U(P_i) = 0.2$ MPa.

Excess molar volume (V^E) was also calculated to correlate the methanol composition with the system association degree, as given below:

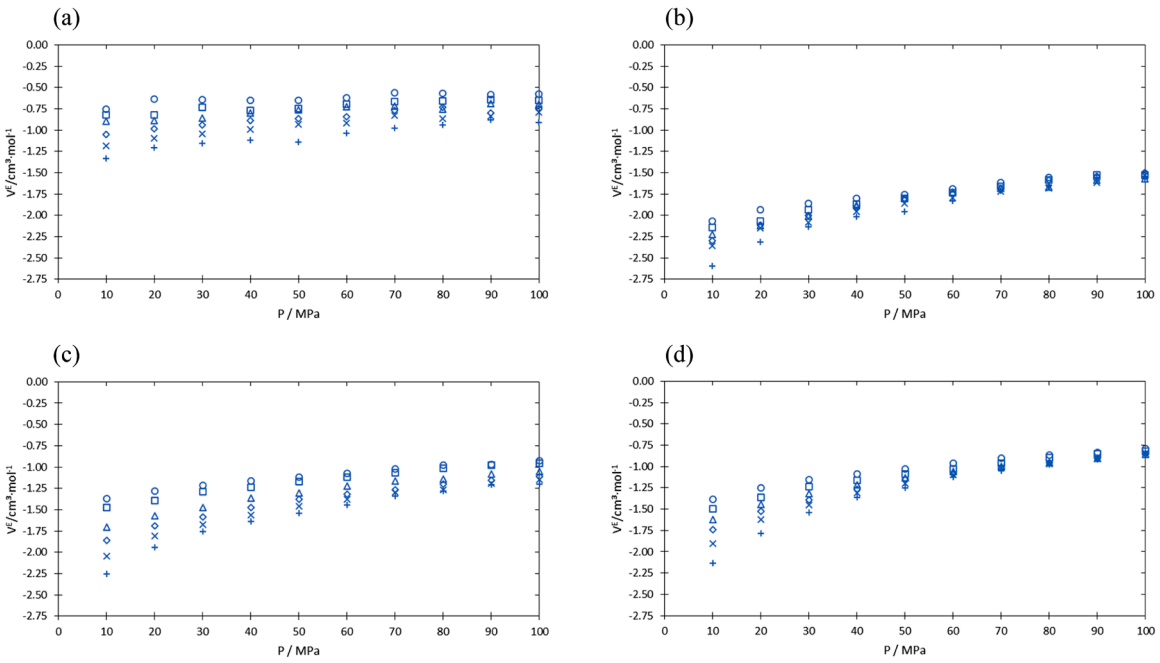

Fig. 2. Excess molar volume (V^E) [$cm^3 \cdot mol^{-1}$] against pressure for IGEPAL CO-720 + methanol mixtures in the following molar compositions: (a) 20.70%; (b) 40.85%; (c) 60.66% and (d) 80.14 % at different temperature. 313.15 K (○), 333.15 K (□), 353.15 K (Δ), 373.15 (◊), 393.15 K (x), 413.15 K (+).

$$V^E = \sum_{i=1}^{n} x_i MW_i \left(\frac{1}{\rho} - \frac{1}{\rho_i}\right) \tag{7}$$

where ρ is the density measured experimentally, and ρ_i is the density of the pure compounds in the same conditions; x_i is the molar fraction of methanol and MW_i is the molecular weight of the *i*-compound in the system. The expanded uncertainty in the excess molar volume $U(V^E)$ was estimated to be 0.006 $cm^3 \cdot mol^{-1}$. The Supplementary Material file depicts the uncertainty calculation procedure.

2.2.4. PC-SAFT modelling

The equation proposed by Gross and Sadowski [19] is based on the statistical associating fluid theory (SAFT) [18], which considers a hard-chain reference fluid composed of hard spheres and can be described in terms of the molar residual Helmholtz energy (a^{res}) by three contributions as the following equation:

$$a^{res} = a^{disp} + a^{assoc} + a^{HC} \tag{8}$$

The contributions of Eq. (8) are: dispersive (a^{disp}), which is based on a modified square-well potential for dispersive interactions, the hard-chain term (a^{HC}), and the association term (a^{assoc}).

The complete description of the PC-SAFT equation can be found elsewhere [18,19]. The PC-SAFT equation needs five pure component parameters for non-associating system description, as given: m – the segment parameter, which states the number of segments in a chain for non-associating molecules; σ is the temperature-independent segment diameter, and ε/k which is the depth of the potential from the square-well potential stating for the segment dispersion energy. For associating molecules, two extra parameters are necessary for a complete description: the energy of association between two sites (ϵ^{AB}/k) and the association volume (κ_{AB}). Additionally, it is also necessary to describe the associating sites. Methanol was described as a 2B, following the criteria defined by Huang and Radosz [40]. The three nonionic surfactants studied here were also modeled as a 2B, following analogous systems studied by Khoshsima & Shahriari [20] with a significant number of ether oxygen, the association energy of the interaction ether O – hydroxyl H is low [41]. The PC-SAFT properties prediction for nonionic surfactant mixtures was successfully implemented elsewhere [20,24,27]. The Berthelot-Lorentz combining rule was utilized for mixtures, allowing one binary interaction parameter (k_{ij}) to correct dispersive interactions [22]. The Wolbach and Sandler [42] combining rules were implemented for cross-association.

The methanol PC-SAFT parameters were obtained elsewhere [22]. The minimization of the following objective function was used to obtain the pure component parameters for the three nonionic surfactants:

$$OF = \sum_{i=1}^{N_P} \left(\frac{\rho_{calc} - \rho_{exp}}{\rho_{exp}}\right)^2 + \sum_{i=1}^{N_P} \left(\frac{P_{calc} - P_{exp}}{P_{exp}}\right)^2 \tag{9}$$

where ρ is the monophasic liquid density, the subscript *calc* is for data obtained through the PC-SAFT equation and *exp* is for experimental values. Usually, the objective function is implemented with vapor pressure and monophasic liquid density minimization. However, compounds with low vapor pressures have limitations for this procedure, and the work of Pakravesh and co-workers [43] proposes the introduction of the system's pressure minimization from PρT data. Nevertheless, the density data is widely applied in the literature [44–47]. The pressure calculation is written as a first-order derivative of the Helmholtz energy, as follows:

$$P = P^{IDEAL} + \rho^2 \left(\frac{\partial A^{res}}{\partial \rho}\right) \tag{10}$$

where P^{IDEAL} is the pressure of the ideal gas reference state. This term was mainly added to the objective function because of the higher deviations from experimental data [43]. Density data was calculated following the algorithm defined in the original work of the equation [19].

The PC-SAFT parameters were compared with the second-order derivative of the Helmholtz residual energy applied in calculating the isobaric expansivity (α_P) and isothermal compressibility (κ_T) coefficients. Tamman-Tait results were used as the standard values for the computation of the deviation presented in Eq. (13). The following equations were used as a function of the pressure derivative for the calculation of the mentioned properties:

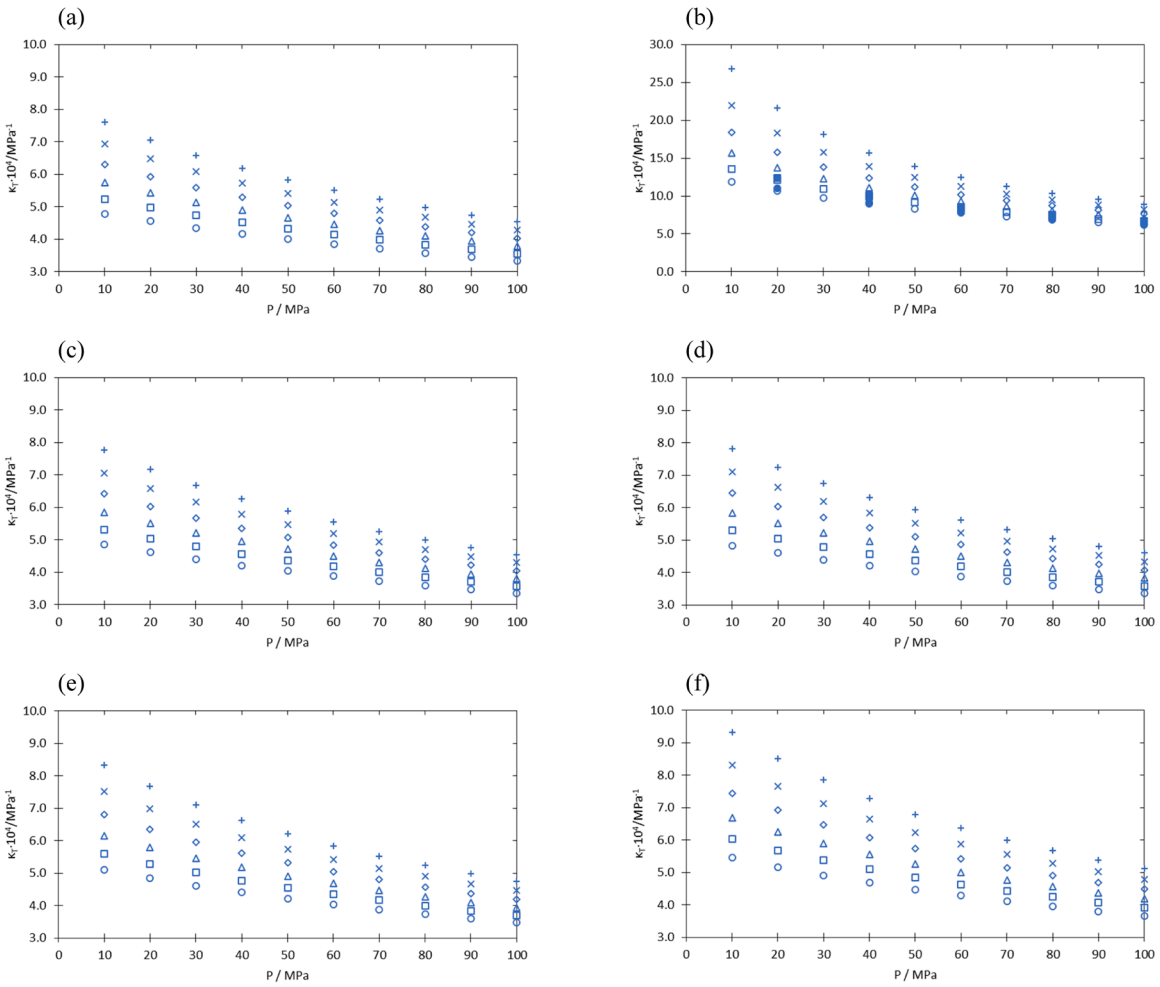

Fig. 3. Isothermal compressibility (κ_T) [MPa^{-1}] against pressure for pure IGEPAL CO-720 (a); methanol (b); and IGEPAL CO-720 + methanol mixture [(c)-(e)]. The molar compositions of methanol are (c) 20.70%, (d) 40.85%, (e) 60.66%, and (f) 80.14 %. Shapes are for temperature: 313.15 K (○), 333.15 K (□), 353.15 K (Δ), 373.15 (◇), 393.15 K (x), 413.15 K (+). Full shapes in methanol data (b) are for literature [36] comparison.

$$k_T^{-1} = \rho \cdot \left(\frac{\partial P}{\partial \rho}\right)_T \tag{11}$$

$$\alpha_P = k_T \cdot \left(\frac{\partial P}{\partial T}\right)_\rho \tag{12}$$

The absolute average relative deviations were calculated using the following equation:

$$\%AARD = \frac{100}{N_{data}} * \sum_{i-1}^{N_{data}} \left| \frac{y_i^{calc} - y_i^{exp}}{y_i^{exp}} \right| \tag{13}$$

where y is the analyzed property: density, pressure, isobaric expansivity, or isothermal compressibility.

3. Results and discussions

3.1. Density measurements and Tammann-Tait correlation

Pure methanol densities experimentally measured were compared to the available data from the NIST database [48] and those given by the Tammann-Tait equation, as provided in Fig. 1(a), while in Fig. 1(b), experimental density data for methanol is overlayed with values available in the literature [49,50]. Experimental data show a good agreement with a maximum standard deviation and absolute relative deviation of 0.85 kg·m^{-3} and 0.034%, respectively. Moreover, Tammann-Tait regression showed a maximum standard deviation of 1.0 kg·m^{-3} and an average absolute relative deviation of 0.043%. Both maximum standard deviations are below the expanded uncertainty for the density (1.7 kg·m^{-3}). The experimentally measured methanol density data are available in Table S1 in the Supplementary Material file. Fig. 1(b) direct comparison among data also shows a good agreement when evaluating the temperature trend of the data.

The regressed Tammann-Tait parameters are presented in Table 2. As Eq. (1) is not composition-dependent, a set of parameters must be obtained for each mixture composition and pure compounds. The standard deviation for each set is lower than the density's expanded uncertainty.

The maximum average absolute relative deviation (%AARD) among the datasets is 0.027%, obtained from pure methanol data. All experimentally measured density data are available in the Supplementary Material (Tables S2 to S4).

Fig. 2 and Tables S5 to S7 from the Supplementary Material show the calculated excess molar volume. A negative deviation was observed in the entire molar range composition, with a negative minimum at a methanol molar composition of 40.85% [Fig. 2(b)] for the IGEPAL CO-520 and CO-720 systems. However, IGEPAL CO-630 presented a peak at 60.0% methanol molar composition. Along isotherms, the mixtures tend to ideality at higher pressures, while the deviation increases with temperature along isobars, as seen in Fig. 2. Similar results were observed at atmospheric pressure for IGEPAL + ethanol mixtures [16].

Moreover, a negative deviation with a peak near 40.00% in methanol molar composition was observed for different mixtures, as observed by

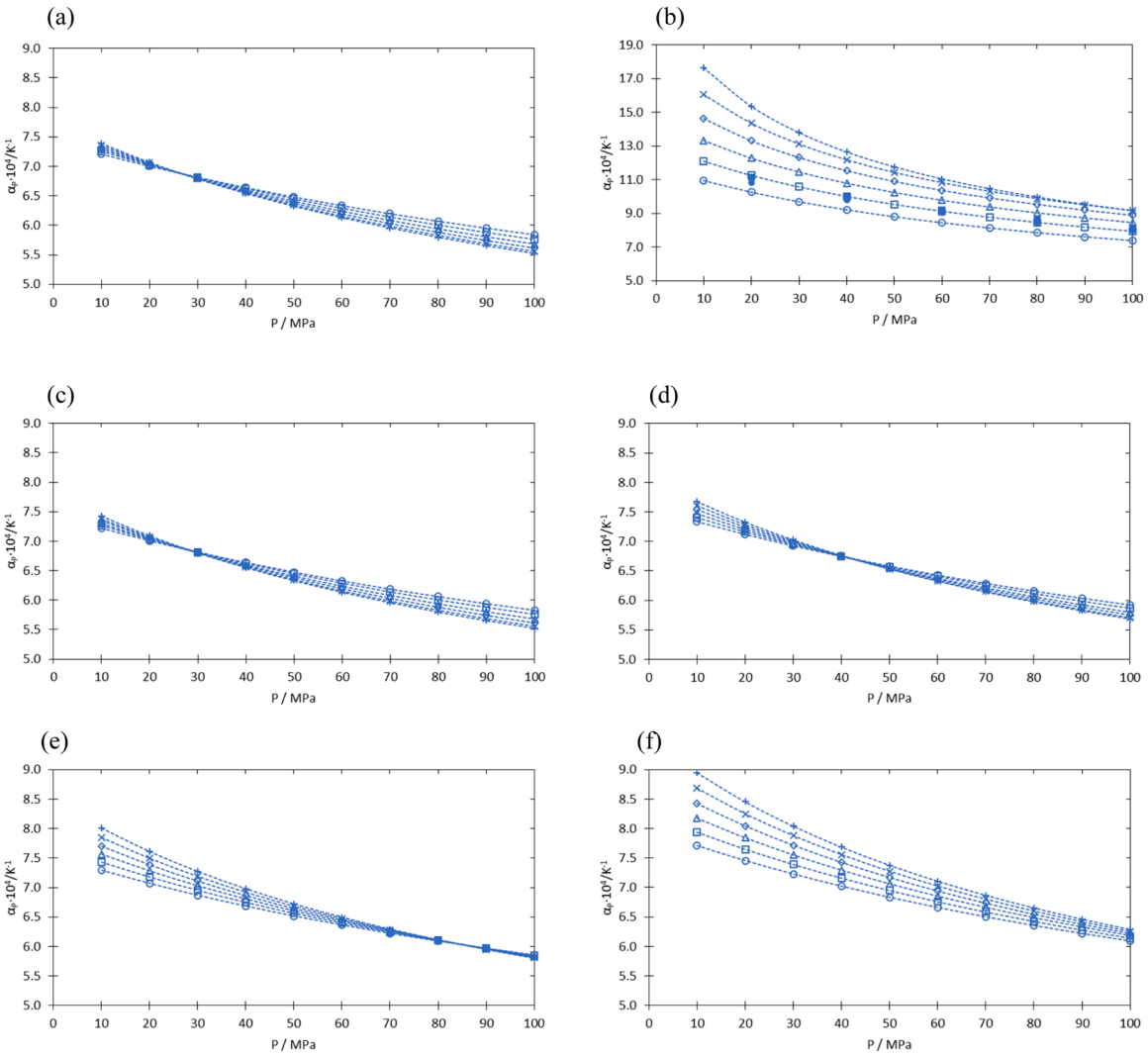

Fig. 4. Isobaric expansivity coefficient (α_p) [K^{-1}] against pressure for pure IGEPAL CO-720 (a); methanol (b); and IGEPAL CO-720 + methanol mixture [(c)-(e)]. The molar compositions of methanol are (c) 20.70%, (d) 40.85%, (e) 60.66%, and (f) 80.14 %. Shapes are for temperature: 313.15 K (○), 333.15 K (□), 353.15 K (Δ), 373.15 (◊), 393.15 K (x), 413.15 K (+). Full circles in methanol data (b) are for literature [36] comparison. Dashed lines are for visual guidance.

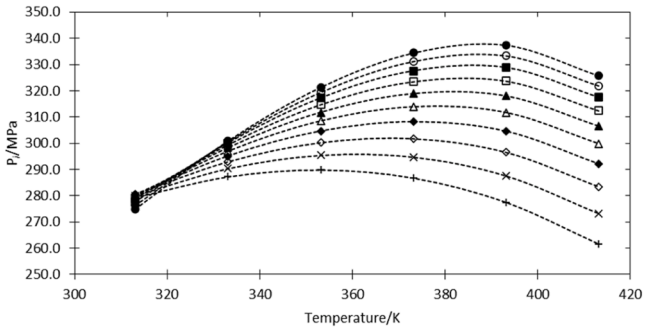

Fig. 5. Internal pressure (P_i) [MPa] against temperature for pure methanol at different pressure conditions, as follows: 10.0 MPa (plus - +); 20.0 MPa (cross - ×); 30.0 MPa (diamond - ◊); 40.0 MPa (solid diamond - ◆); 50.0 MPa (triangle - Δ); 60.0 MPa (solid triangle - ▲); 70.0 MPa (square - □); 80.0 MPa (solid square - ■); 90.0 MPa (circle - ○), and 100.0 MPa (solid circle - ●). Dashed lines are for visual guidance.

Liu et al. [51]. Probably, these results come from the molecular size of methanol, which can cause specific intermolecular interactions justifying the negative excess volume [52,53] and the interactions between hydroxyl – H and ether – O. The oxyethylene unit number seems not to have any influence on the ideality deviation for the mixtures studied here. The lower volume contraction was observed for the composition of 20.70%, which was expected because of the lower contribution from cross-association between methanol molecules and surfactant structure. These results also highlight the cross-association of the molecules, once at surfactant or methanol molar excess the deviation from ideality is lower. Another impact of the methanol structure on the negative excess molar volume is the interstitial accommodation of methanol molecules in the structure of the larger compound (in this case, the surfactants) [54].

As previously mentioned, the isothermal compressibility and the isobaric expansivity were obtained through the analytical derivative of the Tammann-Tait equation, as shown in Eqs. (4) and (5). Fig. 3 depicts the isothermal compressibility (κ_T) for pure IGEPAL CO-720, methanol, and their mixtures, which behave as a regular liquid, presenting an inversely proportional trend with pressure [55]. The complete dataset is in Tables S8 to S11 (Supplementary Material file).

Fig. 4 shows the isobaric expansivity for pure IGEPAL CO-720 and pure methanol and their mixtures. Again, as previously mentioned, this mixture presents as a regular liquid (as the pressure increases, the expansivity decreases). However, a point of inflection against temperature is observed. As the temperature rises, H-bond formation is

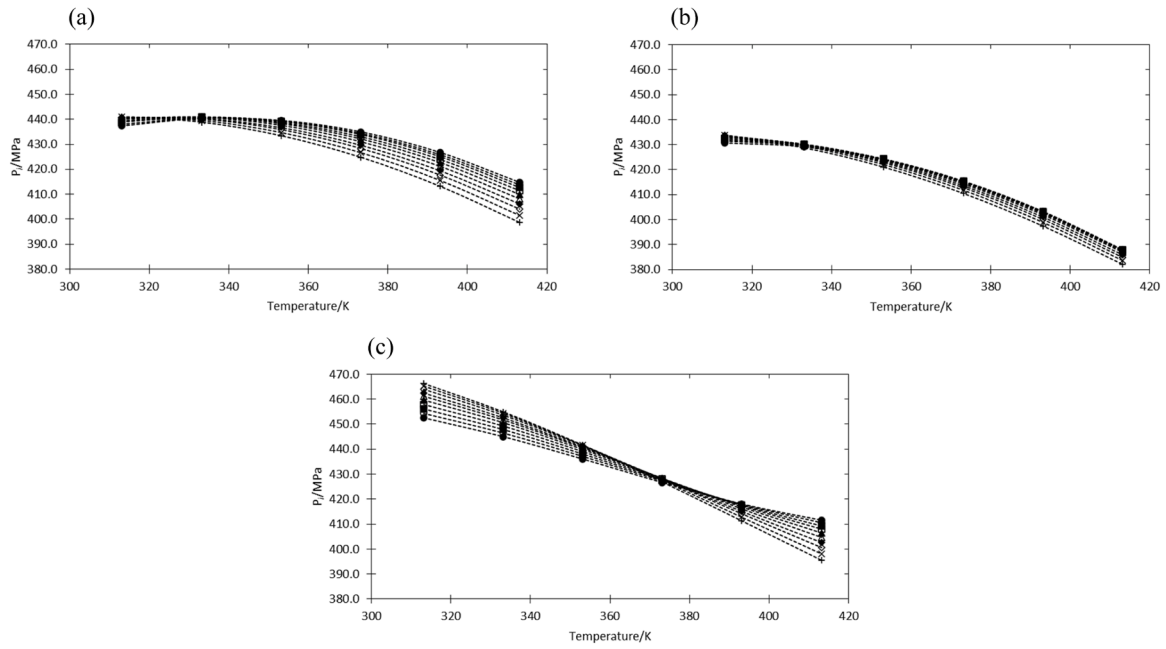

Fig. 6. Internal pressure (P_i) [MPa] against temperature for the mixtures IGEPAL CO-520 + methanol (a) ($x_{methanol}$ = 39.99%); IGEPAL CO-630 + methanol (b) ($x_{methanol}$ = 40.35%); and IGEPAL CO-720 + methanol (c) ($x_{methanol}$ = 40.85%) at different pressure, as follows: 10.0 MPa (plus - +); 20.0 MPa (cross - ×); 30.0 MPa (diamond - ◊); 40.0 MPa (solid diamond - ◆; 50.0 MPa (triangle - Δ); 60.0 MPa (solid triangle - ▲); 70.0 MPa (square - □); 80.0 MPa (solid square - ■); 90.0 MPa (circle - ○); 100.0 MPa (solid circle - ●). Dashed lines are for visual guidance.

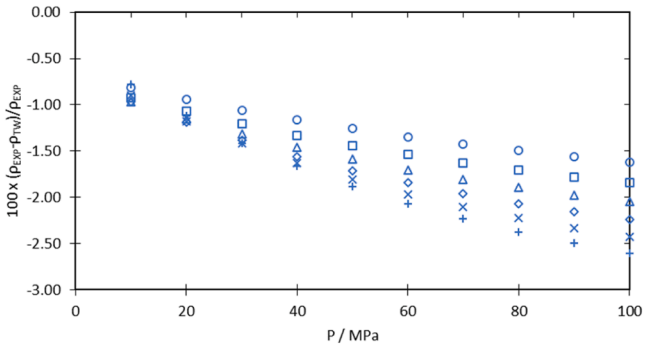

Fig. 7. Deviation of methanol's monophasic liquid density calculated through PC-SAFT equation compared with NIST database at different temperatures. 313.15 K (○), 333.15 K (□), 353.15 K (Δ), 373.15 (◊), 393.15 K (x), 413.15 K (+).

negatively affected, and dispersion forces govern the system's intermolecular interactions [52,56]. Once methanol has a short alkyl chain, pure methanol isobaric expansivity does not show any inflection in the operational conditions studied in this work. This behavior was also observed for all binary mixtures studied here [nonylphenol ethoxylated nonionic surfactant (IGEPAL CO-520, CO-630, and CO-720) + methanol], suggesting that the IGEPAL polyoxyethylene chain length change slightly affects both the isothermal compressibility and the isobaric expansivity. The complete dataset from the Supplementary Material file is available in Tables S12 to S15.

The internal pressure follows an expected trend observed for associating systems. Fig. 5 presents an inflection point at higher pressure conditions, which shows the influence of hydrogen bonds in the internal pressure [57,58], indicating a pressure-dependent inversion point. This behavior could be explained by the H-bond number, which is inversely proportional to the temperature and directly proportional to the pressure [59], and, as temperature increases, the dispersive interactions are dominant. The complete dataset for methanol's internal pressure is available in Table S16 from the Supplementary Material file.

Fig. 6 presents the internal pressure for nonylphenol ethoxylated nonionic surfactant (IGEPAL CO-520, CO-630, and CO-720) + methanol mixtures at a mole composition of 40.00%, where a higher deviation from ideality was observed. At first, along isobars, the internal pressure decreases with temperature. Otherwise, the internal pressure is temperature-independent at lower temperatures. Furthermore, increasing the number of oxyethylene units increases the system's internal pressure when comparing the same temperature pressure and composition conditions, probably because of the more significant number of ether oxygens. However, the tendency to decrease with temperature is strengthened because of the weaker interactions of the hydroxyl hydrogen with the ether oxygen. The complete dataset for internal pressure for all systems studied here is in the Supplementary Material file (Tables S16 to S19).

Table 3
Pure component parameters for PC-SAFT equation of state.

i–Compound	*Parameters*					*%AARD*	*T [K] range*
	m_i	σ_i (Å)	*ε_i/k* (K)	*κ_(AB_i)*	*ε_iÅB/k* (K)	*ρ – monophasic liquid density*	
Methanol*	1.5255	3.2300	188.90	0.0352	2899.5	1.61	313.15 – 413.15
IGEPAL CO-520	19.5379	3.1646	256.85	0.9491	2987.3	0.093	
IGEPAL CO-630	27.4536	3.1415	255.81	0.8385	2994.1	0.090	
IGEPAL CO-720	32.8497	3.1538	259.74	0.9623	2993.3	0.094	

* Methanol's parameters were obtained from the work of Gross and Sadowski [22]. Other parameters were fitted in this work.

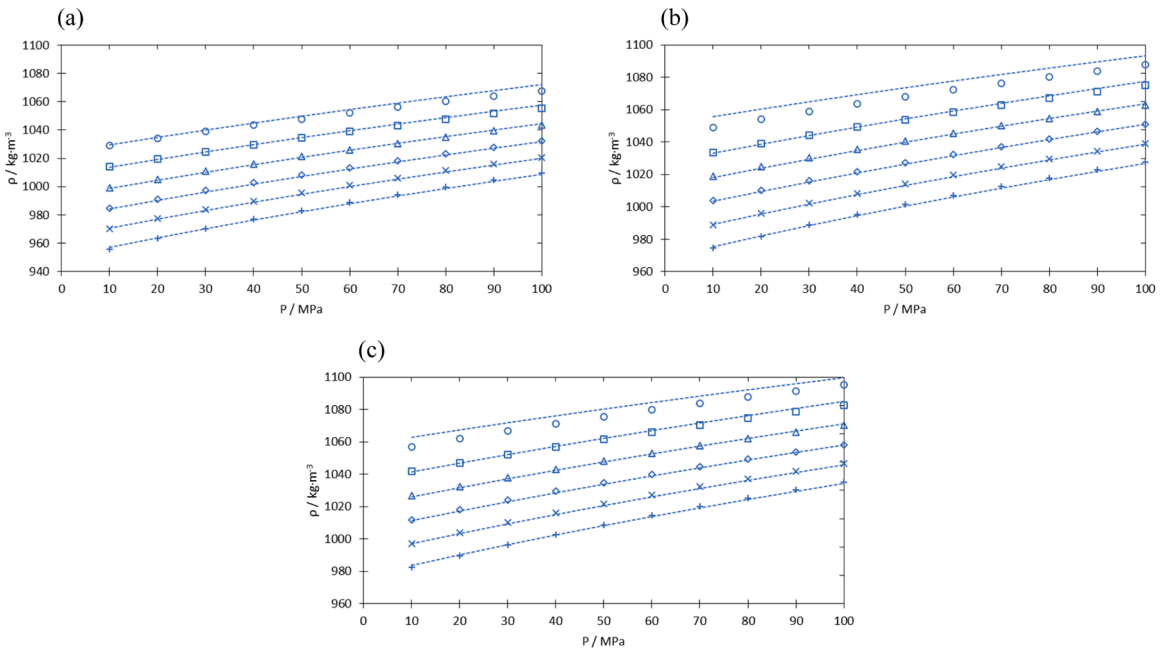

Fig. 8. Experimental density (shapes) and PC-SAFT calculated (dashed lines) for pure (a) IGEPAL CO-520, (b) IGEPAL CO-630, and (c) IGEPAL CO-720 at different temperatures: 313.15 K (○), 333.15 K (□), 353.15 K (Δ), 373.15 (◊), 393.15 K (x), 413.15 K (+). Dashed lines are used to calculate the density using the PCSAFT equation of state.

Table 4
Absolute average relative deviation (%AARD) for all IGEPAL + methanol mixtures monophasic liquid density at all temperatures calculated in this work.

	%AARD					
Temperature / K	IGE	IGE 80 – MetOH 20	IGE 60 – MetOH 40	IGE 40 – MetOH 60	IGE 20 – MetOH 80	MetOH
	IGEPAL CO – 520					
313.15	0.21	0.12	0.40	0.25	0.66	1.27
333.15	0.08	0.14	0.51	0.17	0.64	1.45
353.15	0.05	0.20	0.56	0.14	0.66	1.59
373.15	0.06	0.23	0.55	0.15	0.73	1.71
393.15	0.07	0.22	0.48	0.17	0.84	1.80
413.15	0.08	0.19	0.40	0.24	0.94	1.86
	IGEPAL CO – 630					
313.15	0.20	0.15	0.13	0.14	0.35	
333.15	0.09	0.09	0.09	0.10	0.28	
353.15	0.06	0.10	0.11	0.10	0.27	
373.15	0.06	0.10	0.14	0.10	0.29	
393.15	0.06	0.08	0.15	0.09	0.33	
413.15	0.07	0.05	0.14	0.08	0.40	
	IGEPAL CO – 720					
313.15	0.22	0.11	0.29	0.33	0.68	
333.15	0.08	0.11	0.43	0.44	0.74	
353.15	0.05	0.19	0.50	0.52	0.75	
373.15	0.06	0.23	0.51	0.55	0.71	
393.15	0.07	0.24	0.51	0.53	0.64	
413.15	0.07	0.23	0.47	0.49	0.55	

$$\%AARD = \frac{100}{N_{data}} * \sum_{i-1}^{N_{data}} \left| \frac{\rho_i^{calc} - \rho_i^{exp}}{\rho_i^{exp}} \right|.$$

3.2. PC-SAFT modeling

Fig. 7 compares methanol density obtained from the PC-SAFT equation of state at pressures up to 100.0 MPa (for T = 313.15 – 413.15 K) using the parameters from Gross and Sadowski [22] and data available at the NIST database [48]. The equation predicts density with good agreement, showing a maximum deviation at the pressure near 100.0 MPa for all temperatures. Moreover, the temperature is also directly related to the deviation, as shown in Figure 7; the higher the temperature, the higher the error.

The regressed parameters for pure IGEPAL are shown in Table 3. The pure components' densities are presented in Fig. 8 against PC-SAFT calculation data, showing a good agreement with experimental measurements, with the following maximum deviation (%AARD): 0.21%, 0.20%, and 0.22% for IGEPAL CO-520, CO-630, and CO-720 respectively at 313.15 K of. These results could be related to the high association at lower temperatures. Furthermore, the parameters follow a direct trend with the molecular mass of the compounds, as also observed in the literature results [20,21,23,44–46].

The association parameters (association volume κ_{AB} and energy of association ε^{AB}/k) presented similar values because of the compound's similarity. Furthermore, the association volume (κ_{AB}) stands for the

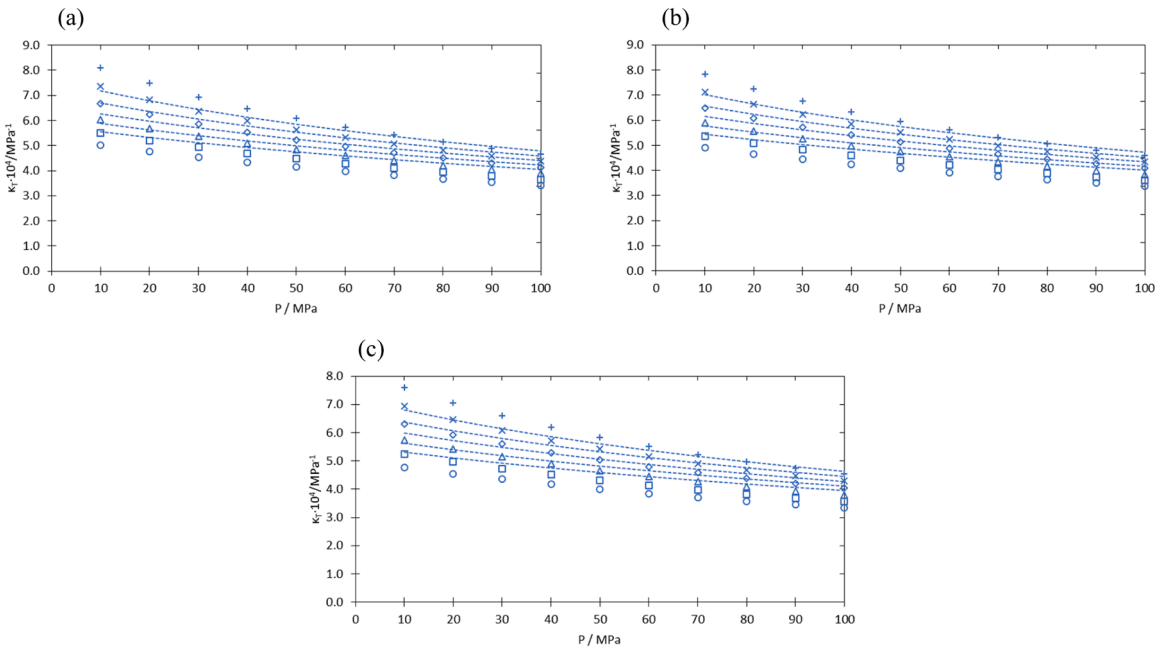

Fig. 9. Experimental isothermal compressibility (κ_T) [MPa^{-1}] (shapes) compared with PC-SAFT equation calculations (dashed lines) for pure (a) IGEPAL CO-520, (b) IGEPAL CO-630, and (c) IGEPAL CO-720 at different temperatures: 313.15 K (○), 333.15 K (□), 353.15 K (Δ), 373.15 (◊), 393.15 K (x), 413.15 K (+).

Table 5
Absolute average relative deviation (%AARD) for all IGEPAL's derivative properties estimated using the PC-SAFT equation of state and the set of parameters for isothermal compressibility and isobaric expansivity.

	%AARD	
Temperature / K	α_P	κ_T
	IGEPAL CO – 520	
313.15	14.40	9.61
333.15	8.98	6.41
353.15	5.02	4.23
373.15	3.12	3.48
393.15	2.54	3.70
413.15	2.53	4.55
	IGEPAL CO – 630	
313.15	14.02	9.76
333.15	8.64	6.52
353.15	4.72	4.16
373.15	2.82	3.28
393.15	2.24	3.38
413.15	2.31	4.10
	IGEPAL CO – 720	
313.15	15.41	10.03
333.15	9.59	6.57
353.15	5.20	4.01
373.15	2.95	3.12
393.15	2.28	3.33
413.15	2.67	4.13

$$\%AARD = \frac{100}{N_{data}} * \sum_{i-1}^{N_{data}} \left| \frac{y_i^{calc} - y_i^{exp}}{y_i^{exp}} \right|.$$

where y is α_P or κ_T.

distance between the association sites in a square well potential analogous interaction [18], which for pure IGEPAL was expected to be high due to the high level of association for the pure compounds, such as in analogous results from Avlund and co-workers [24]. The results obtained for the energy of association also highlight the similarity of the compounds' interactions and the strength of the self-association for the pure nonionic surfactants.

The simulation results are presented in Table 4. Although the H-bonds between hydroxyl groups and the oxygens from the ethoxylated chain on IGEPALS present less energy [41], it is very likely that they contribute to increasing the nonideality for the mixtures studied here by increasing the number of associating sites, as can be seen from the higher deviation of IGEPAL CO-720 + methanol simulation results. Also, the short alkyl chain of methanol molecules could potentialize the cross-association of the mixtures, with both hydroxyl groups and the oxygens from the ethoxylated chain in IGEPAL's structure. The pressure calculation deviations are expected to be high, as pointed out by other authors [46,60,61], which was one of the main reasons for its inclusion in the parametrization process [43].

The calculated isothermal compressibility with PC-SAFT parameters compared with Tamman-Tait calculations follows in Fig. 9. Previous works report that equations of state tend to give poor predictions for such properties [62,63] once they deal with the second-order derivative of the residual Helmholtz energy. The results obtained here agreed with more accurate data from the Tamman-Tait equation, which could validate the set of pure compound parameters regressed in this work. The average deviations for all data are available in Table 5. Deviations for each temperature and pressure are available in the Supplementary Material file, Tables S20 and S21.

4. Conclusions

Experimental densities for nonylphenol ethoxylated nonionic surfactant (IGEPAL CO-520, CO-630, and CO-720) + methanol mixtures in a wide range of composition for $T = 313.15$–413.15 K and pressure up to 100 MPa. These mixtures behave as highly associative systems, as regular liquids with the predominance of attractive intermolecular forces. The polyethoxylated chain length influences the volumetric properties. From internal pressure data and the PC-SAFT equation calculations, this system has a high cohesive force when the ethoxylate unit number increases. As expected, the PC-SAFT equation and the Tammann-Tait correlation are suitable for modeling alkylphenol ethoxylated surfactants.

CRediT authorship contribution statement

Moacir Frutuoso Leal da Costa: Writing – review & editing, Writing

– original draft, Validation, Methodology, Investigation. **Hugo Andersson de Medeiros:** Writing – original draft, Validation, Methodology. **Alanderson Arthu Araújo Alves:** Methodology, Investigation. **Lucas Henrique Gomes de Medeiros:** Methodology, Investigation. **Filipe Xavier Feitosa:** Writing – review & editing, Writing – original draft, Supervision, Conceptualization. **Hosiberto Batista De Sant'Ana:** Writing – review & editing, Writing – original draft, Supervision, Resources, Funding acquisition, Conceptualization.

Declaration of competing interest

The authors declare that they have no known competing financial interests or personal relationships that could have appeared to influence the work reported in this paper.

Data availability

Data will be made available on request.

Acknowledgment

The authors are grateful to CNPq (Conselho Nacional de Desenvolvimento Científico e Tecnológico. Brasil) and CAPES (Coordenação de Aperfeiçoamento de Pessoal de Nível Superior. Brasil). The authors are also thankful for the financial support of the Human Resources Program from Agência Nacional de Petróleo, Gás Natural e Biocombussstíveis – PRH-ANP, supported with resources provided by investments from oil companies which are qualified in the P, D&I clause from the ANP resolution nº 50/2015.

Supplementary materials

Supplementary material associated with this article can be found, in the online version, at doi:10.1016/j.fluid.2024.114076.

References

[1] T.F. Tadros, Applied Surfactants: Principles and Applications, Blackwell Science Publ, Oxford, 2005.
[2] R.C. Nelson, Application of surfactants in the petroleum industry, J. Am. Oil. Chem. Soc. 59 (1982) 823A–826A, https://doi.org/10.1007/BF02634448.
[3] K.M. Heyob, J. Blotevogel, M. Brooker, M.V. Evans, J.J. Lenhart, J. Wright, R. Lamendella, T. Borch, P.J. Mouser, Natural attenuation of nonionic surfactants used in hydraulic fracturing fluids: degradation rates, pathways, and mechanisms, Environ. Sci. Technol. 51 (2017) 13985–13994, https://doi.org/10.1021/acs.est.7b01539.
[4] J.M.A. Godoi, P.H.L. dos Santos Matai, Enhanced oil recovery with carbon dioxide geosequestration: first steps at Pre-salt in Brazil, J. Pet. Explor. Prod. Technol. 11 (2021) 1429–1441, https://doi.org/10.1007/s13202-021-01102-8.
[5] A.M. Hassan, E.W. Al-Shalabi, W. Alameri, M.S. Kamal, S. Patil, S.M. Shakil Hussain, Manifestations of surfactant-polymer flooding for successful field applications in carbonates under harsh conditions: a comprehensive review, J. Pet. Sci. Eng. 220 (2023) 111243, https://doi.org/10.1016/J.PETROL.2022.111243.
[6] D. França, D.M. Coutinho, T.A. Barra, R.S. Xavier, D.A. Azevedo, Molecular-level characterization of Brazilian pre-salt crude oils by advanced analytical techniques, Fuel 293 (2021) 120474, https://doi.org/10.1016/J.FUEL.2021.120474.
[7] T.Y. Makogon, Initial diagnosis and solution of flow assurance production problems in operations. Handbook of Multiphase Flow Assurance, Elsevier, 2019, pp. 35–42, https://doi.org/10.1016/B978-0-12-813062-9.00002-6.
[8] A.A. Umar, I.B.M. Saaid, A.A. Sulaimon, R.B.M. Pilus, A review of petroleum emulsions and recent progress on water-in-crude oil emulsions stabilized by natural surfactants and solids, J. Pet. Sci. Eng. 165 (2018) 673–690, https://doi.org/10.1016/j.petrol.2018.03.014.
[9] Nagamune. Nishikido, Phase equilibria of nonionic surfactant-water systems as a function of temperature and pressure: effect of mixing of surfactants, J. Coll. Interf. Sci. 136 (2) (1990) 401–407.
[10] J.L. Li, D.S. Bai, B.H. Chen, Effects of additives on the cloud points of selected nonionic linear ethoxylated alcohol surfactants, Coll. Surf. a Physicochem. Eng. Asp. 346 (2009) 237–243, https://doi.org/10.1016/J.COLSURFA.2009.06.020.
[11] M. Kahlweit, R. Strey, G. Busse, Effect of alcohols on the phase behavior of microemulsions, J. Phys. Chem. 95 (13) (1991) 5344–5352.
[12] J.F. Scamehorn, An overview of phenomena involving surfactant mixtures, in: 1986: pp. 1–27. https://doi.org/10.1021/bk-1986-0311.ch001.
[13] R.R. Balmbra, J.S. Clunie, J.M. Corkill, J.F. Goodman, Effect of temperature on the micelle size of a homogeneous non-ionic detergent, Transact. Faraday Soc. 58 (1962) 1661, https://doi.org/10.1039/tf9625801661.
[14] Tiren Gu, P.A. Galera-Gomez, The effect of different alcohols and other polar organic additives on the cloud point of Triton X-100 in water, Coll. Surf. A: Physicochem. Engin. Asp. 147 (3) (1999) 365–370.
[15] S. Kumar, A. Mandal, Investigation on stabilization of CO2 foam by ionic and nonionic surfactants in presence of different additives for application in enhanced oil recovery, Appl. Surf. Sci. 420 (2017) 9–20, https://doi.org/10.1016/J.APSUSC.2017.05.126.
[16] C.L. Paiva, R.S. Pinheiro, F.X. Feitosa, H.B. de Sant'Ana, Viscosity and density of binary mixtures of Ethanol + Igepal (CO-520, CO-630, CO-720, and CA-720), J. Chem. Eng. Data 64 (2019) 594–602, https://doi.org/10.1021/acs.jced.8b00793.
[17] C.L. Paiva, R.S. Pinheiro, F.X. Feitosa, H. Batista de Sant'Ana, Viscosity and Density of Binary Mixtures of Toluene + Igepal (CO-520, CO-630, CO-720, and CA-720) at T = 293.15–333.15K and Atmospheric Pressure, J. Chem. Eng. Data 65 (2020) 540–548, https://doi.org/10.1021/acs.jced.9b00718.
[18] W.G. Chapman, K.E. Gubbins, G. Jackson, M. Radosz, New reference equation of state for associating liquids, Ind. Eng. Chem. Res. 29 (1990) 1709–1721, https://doi.org/10.1021/ie00104a021.
[19] J. Gross, G. Sadowski, Perturbed-chain SAFT: an equation of state based on a perturbation theory for chain molecules, Ind. Eng. Chem. Res. 40 (2001) 1244–1260, https://doi.org/10.1021/ie0003887.
[20] A. Khoshsima, R. Shahriari, Modeling study of the phase behavior of mixtures containing non-ionic glycol ether surfactant, J. Mol. Liq. 230 (2017) 529–541, https://doi.org/10.1016/j.molliq.2017.01.058.
[21] A. Grenner, G.M. Kontogeorgis, N. von Solms, M.L. Michelsen, Application of PC-SAFT to glycol containing systems - PC-SAFT towards a predictive approach, Fluid. Phase Equilib. 261 (2007) 248–257, https://doi.org/10.1016/j.fluid.2007.04.025.
[22] J. Gross, G. Sadowski, Application of the perturbed-chain saft equation of state to associating systems, Ind. Eng. Chem. Res. 41 (2002) 5510–5515, https://doi.org/10.1021/ie010954d.
[23] J. Gross, G. Sadowski, Modeling polymer systems using the perturbed-chain statistical associating fluid theory equation of state, Ind. Eng. Chem. Res. 41 (2002) 1084–1093, https://doi.org/10.1021/ie010449g.
[24] A.S. Avlund, G.M. Kontogeorgis, M.L. Michelsen, Application of simplified PC-SAFT to glycol ethers, Ind. Eng. Chem. Res. 51 (2012) 547–555, https://doi.org/10.1021/ie2011406.
[25] Z.S. Baird, P. Uusi-Kyyny, J.P. Pokki, E. Pedegert, V. Alopaeus, Vapor pressures, densities, and PC-SAFT Parameters for 11 bio-compounds, Int. J. Thermophys. 40 (2019), https://doi.org/10.1007/s10765-019-2570-9.
[26] N. Von Solms, I.A. Kouskoumvekaki, M.L. Michelsen, G.M. Kontogeorgis, Capabilities, limitations and challenges of a simplified PC-SAFT equation of state, Fluid. Phase Equilib. 241 (2006) 344–353, https://doi.org/10.1016/j.fluid.2006.01.001.
[27] I. Stoychev, J. Galy, B. Fournel, P. Lacroix-Desmazes, M. Kleiner, G. Sadowski, Modeling the phase behavior of PEO-PPO-PEO surfactants in carbon dioxide using the PC-SAFT equation of state: application to dry decontamination of solid substrates, J. Chem. Eng. Data 54 (2009) 1551–1559, https://doi.org/10.1021/je800875k.
[28] A.M. Chacon Valero, F.X. Feitosa, H. Batista De Sant'ana, Density and volumetric behavior of binary CO2+ n-Decane and Ternary CO2+ n-Decane + Naphthalene systems at high pressure and high temperature, J. Chem. Eng. Data 65 (2020) 3499–3509, https://doi.org/10.1021/acs.jced.0c00090.
[29] A.M. Chacón Valero, C.A. Alves, F.X. Feitosa, H.B. De Sant'Ana, Density and volumetric behavior of Ternary CO2+ n-Decane + cis-Decalin (or + trans-Decalin) mixtures at high pressure and high temperature, J. Chem. Eng. Data 66 (2021) 1684–1693, https://doi.org/10.1021/acs.jced.0c00989.
[30] L.H.G. De Medeiros, A.A.A. Alves, F.X. Feitosa, H.B. De Sant'ana, High-pressure and high-temperature density data, derivative properties, and group contribution models applied for 1-Methyl-3-octylimidazolium Trifluoromethanesulfonate, 1-Butyl-1-methylpyrrolidinium Dicyanamide, and 1-Ethyl-3-methylimidazolium Acetate Ionic Liquids, J. Chem. Eng. Data (2022), https://doi.org/10.1021/acs.jced.2c00036.
[31] L.H.G. de Medeiros, A.A.A. Alves, F.X. Feitosa, H.B. de Sant'Ana, Cation effect on bis(trifluoromethylsulfonyl)imide-based ionic liquids with triethylsulfonium, 1,2-dimethyl-3-propylimidazolium, 1-methyl-1-propylpyrrolidinium, and 1-butyl-2,3-dimethylimidazolium density at high pressure, J. Mol. Liq. 354 (2022), https://doi.org/10.1016/j.molliq.2022.118851.
[32] J.H. Dymond, R. Malhotra, The Tait equation: 100 years on, Int. J. Thermophys. 9 (1988) 941–951.
[33] G. Tammann, Ueber die Abhängigkeit der Volumina von Lösungen vom Druck, Zeitschrift Für Physikalische Chemie 17U (1895) 620–636, https://doi.org/10.1515/zpch-1895-1738.
[34] T. Hofman, A. Gołdon, A. Nevines, T.M. Letcher, Densities, excess volumes, isobaric expansivity, and isothermal compressibility of the (1-ethyl-3-methylimidazolium ethylsulfate + methanol) system at temperatures (283.15 to 333.15) K and pressures from (0.1 to 35) MPa, J. Chem. Thermody. 40 (2008) 580–591, https://doi.org/10.1016/j.jct.2007.11.011.
[35] H. Hoang, G. Galliero, Predictive Tait equation for non-polar and weakly polar fluids: applications to liquids and liquid mixtures, Fluid. Phase Equilib. 425 (2016) 143–151, https://doi.org/10.1016/J.FLUID.2016.05.026.
[36] T. Sun, S.N. Biswas, N.J. Trappenlers, C.A. Ten Beldam, Acoustic and thermodynamic properties of methanol from 273 to 333K and at Pressures to 280MPa, 1988. https://pubs.acs.org/sharingguidelines.

[37] J.M. Prausnitz, R.N. Lichtenthaler, E.G. De Azevedo, Molecular Thermodynamics of Fluid Phase Equilibria, Pearson Education, 1998.
[38] E. Zorębski, M. Musiał, M. Dzida, Relation between temperature–pressure dependence of internal pressure and intermolecular interactions in ionic liquids – comparison with molecular liquids, J. Chem. Thermody. 131 (2019) 347–359, https://doi.org/10.1016/j.jct.2018.11.007.
[39] J.J. Moré, The Levenberg-Marquardt algorithm: implementation and theory, in: 1978: pp. 105–116. https://doi.org/10.1007/BFb0067700.
[40] S.H. Huang, M. Radosz, Equation of state for small, large, polydisperse, and associating molecules, 1990. https://pubs.acs.org/sharingguidelines.
[41] J.P.M. Lommerse, S.L. Price, R. Taylor, Hydrogen bonding of Carbonyl, Ether, and Ester Oxygen atoms with Alkanol Hydroxyl groups, J. Comput. Chem. 18 (1997).
[42] J.P. Wolbach, S.I. Sandler, Using molecular orbital calculations to describe the phase behavior of Hydrogen-bonding fluids, Ind. Eng. Chem. Res. 36 (10) (1997) 4041–4051.
[43] A. Pakravesh, F. Zarei, H. Zarei, PρT parameterization of SAFT equation of state: developing a new parameterization method for equations of state, Fluid. Phase Equilib. 538 (2021) 113024, https://doi.org/10.1016/j.fluid.2021.113024.
[44] R. Aitbelale, Y. Chhiti, F.E.M. hamdi Alaoui, A. Sahib Eddine, N. Munõz Rujas, F. Aguilar, High-pressure soybean oil biodiesel density: experimental measurements, correlation by Tait equation, and perturbed chain SAFT (PC-SAFT) Modeling, J. Chem. Eng. Data 64 (2019) 3994–4004, https://doi.org/10.1021/acs.jced.9b00391.
[45] R. Mohammadkhani, A. Paknejad, H. Zarei, Thermodynamic properties of amines under high temperature and pressure: experimental results correlating with a new modified tait-like equation and PC-SAFT, Ind. Eng. Chem. Res. 57 (2018) 16978–16988, https://doi.org/10.1021/acs.iecr.8b04732.
[46] Z. Mokhtari, A. Pakravesh, H. Zarei, High-pressure densities of 2-(dimethylamino) ethanol and 2-(diethylamino) ethanol: measurement and modeling with new modified Tait and PC-SAFT equations of state, Fluid. Phase Equilib. 572 (2023), https://doi.org/10.1016/j.fluid.2023.113825.
[47] L.F. Zubeir, C. Held, G. Sadowski, M.C. Kroon, PC-SAFT modeling of CO2 solubilities in deep eutectic solvents, J. Phy. Chem. B 120 (2016) 2300–2310, https://doi.org/10.1021/acs.jpcb.5b07888.
[48] E.W. Lemmon, M.O. McLinde, D.G. Friend, Thermophysical properties of fluid systems, in: NIST Chemistry WebBook, NIST Standard Reference Database Number 69, 2018.
[49] H.W. Xiang, A. Laesecke, M.L. Huber, A new reference correlation for the viscosity of methanol, J. Phys. Chem. Ref. Data 35 (2006) 1597–1620, https://doi.org/10.1063/1.2360605.
[50] I.M. Abdulagatov, A. Tekin, J. Safarov, A. Shahverdiyev, E. Hassel, High-pressure densities and derived volumetric properties (excess, apparent, and partial molar volumes) of binary mixtures of {methanol (1)+[BMIM][BF4] (2)}, J. Chem. Thermody. 40 (2008) 1386–1401, https://doi.org/10.1016/j.jct.2008.05.005.
[51] J. Liu, X. Qi, L. Li, N. Chang, J. Wei, D. Fang, Z. Zhang, Physical properties and its estimation of binary mixtures of ether-functionalized ionic liquids [C<inf>2</inf>2O1IM][NTF<inf>2</inf>] with alcohols, J. Chem. Eng. Data 65 (2020) 5176–5183, https://doi.org/10.1021/acs.jced.0c00298.
[52] L. Cai, J. Yin, X. Wang, Density and viscosity investigation for binary mixtures of Polyoxymethylene Dimethyl Ethers with 1-Propanol, 1-Butanol, and 1-Pentanol, J. Chem. Eng. Data 67 (2022) 334–345, https://doi.org/10.1021/acs.jced.1c00878.
[53] A. Pal, R. Gaba, H. Kumar, Acoustic, viscometric, and spectroscopic studies of Dipropylene Glycol Monopropyl Ether with n-Alkanols at temperatures of 288.15, 298.15, and 308.15K, J. Solut. Chem. 40 (2011) 786–802, https://doi.org/10.1007/s10953-011-9688-0.
[54] M.N. Roy, A. Sinha, B. Sinha, Excess molar volumes, viscosity deviations and isentropic compressibility of binary mixtures containing 1,3-Dioxolane and Monoalcohols at 303.15K, J. Solut. Chem. 34 (2005) 1311–1325, https://doi.org/10.1007/s10953-005-8022-0.
[55] A.A.A. Alves, L.H.G. De Medeiros, F.X. Feitosa, H.B. De Sant'Ana, Thermodynamic properties of biodiesel and petrodiesel blends at high pressure and high temperature and a new model for density prediction, J. Chem. Eng. Data 67 (2022) 607–621, https://doi.org/10.1021/acs.jced.1c00918.
[56] A. Pal, R. Gaba, Densities, excess molar volumes, speeds of sound and isothermal compressibilities for {2-(2-hexyloxyethoxy)ethanol + n-alkanol} systems at temperatures between (288.15 and 308.15) K, J. Chem. Thermody. 40 (2008) 750–758, https://doi.org/10.1016/j.jct.2008.01.015.
[57] M.J. Dávila, R. Alcalde, M. Atilhan, S. Aparicio, PρT measurements and derived properties of liquid 1-alkanols, J. Chem. Thermody. 47 (2012) 241–259, https://doi.org/10.1016/j.jct.2011.10.023.
[58] V.N. Kartsev, S.N. Shtykov, The temperature dependence of internal pressure in liquids separation, preconcentration and determination of biologically active substances with application of solid and liquid nanoobjects as toolsof chemical analysis view project synthesis, modification and application of magnetic nanoparticles for preconcentration and determination of biologically active substances view project, 2002. https://www.researchgate.net/publication/259310390.
[59] E. Guàrdia, J. Martí, J.A. Padró, L. Saiz, A.V. Komolkin, Dynamics in hydrogen bonded liquids: water and alcohols, J. Mol. Liq. 96–97 (2002) 3–17. https://doi.org/10.1016/S0167-7322(01)00342-7.
[60] H. Zarei, V. Keley, PρT measurement and PC-SAFT modeling of N, N-dimethyl formamide, N -methyl formamide, N, N-dimethyl acetamide, and ethylenediamine from T = (293.15–423.15) K and pressures up to 35MPa, Fluid. Phase Equilib. 427 (2016) 583–593, https://doi.org/10.1016/j.fluid.2016.08.014.
[61] A. Paknejad, R. Mohammadkhani, H. Zarei, experimental high-temperature, high-pressure density measurement and perturbed-chain statistical associating fluid theory modeling of Dimethyl Sulfoxide, Isoamyl Acetate, and Benzyl alcohol, J. Chem. Eng. Data 64 (2019) 5174–5184, https://doi.org/10.1021/acs.jced.9b00396.
[62] T. Lafitte, D. Bessieres, M.M. Piñeiro, J.-L. Daridon, Simultaneous estimation of phase behavior and second-derivative properties using the statistical associating fluid theory with variable range approach, J. Chem. Phys. 124 (2006), https://doi.org/10.1063/1.2140276.
[63] A. Jamali, H. Behnejad, Observations regarding the first and second order thermodynamic derivative properties of non-polar and light polar fluids by perturbed chain-SAFT equations of state, Cryogenics. (Guildf) 99 (2019) 78–86, https://doi.org/10.1016/j.cryogenics.2019.03.002.